Supporting information for

Fluorescent Hydrogels with Emission Enhancement and CPL-Activity Depending on Gelation States

Yongjie Zhang,[a] Yu-Ming Sun,[a] Gonghui Li,[b] Meiyan Du,[b] Ning Sheng,[a] Jinglin Shen*[b]

[a] *School of Chemistry, Chemical Engineering and Materials, Jining University, Qufu, Shandong, 273155, P. R. China*

[b] *School of Chemistry and Chemical Engineering, Qufu Normal University, Qufu, Shandong, 273165, P. R. China*

*E-mail: jinglinshen@163.com

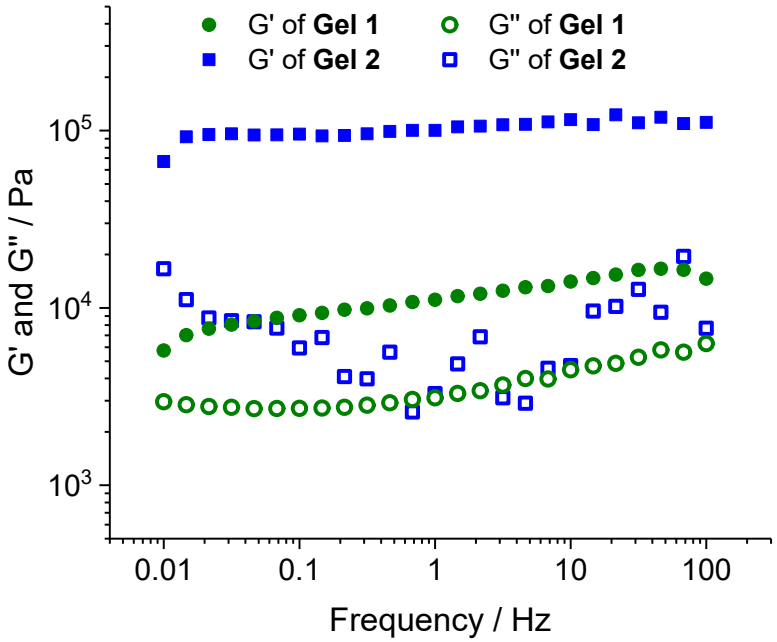

Figure S1. Rheological profiles (G' and G'') of **Gel 1** and **Gel 2** *versus* frequency at fixed shear stress of 1 Pa.

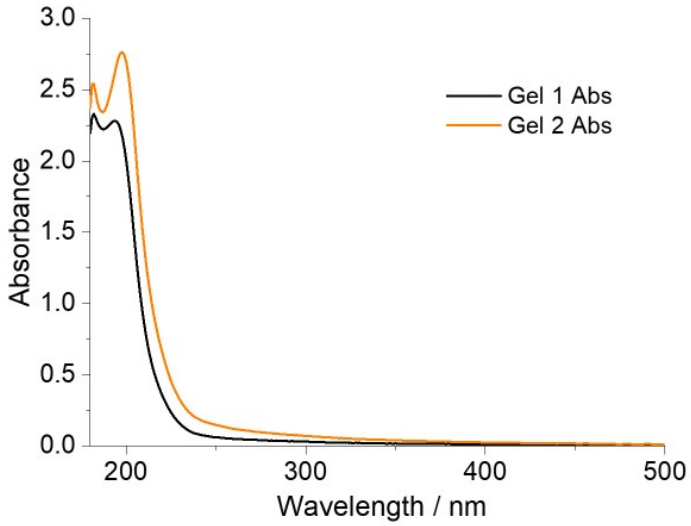

Figure S2. UV/Vis absorption spectra for different gelation states of palmitoyl pentapeptide

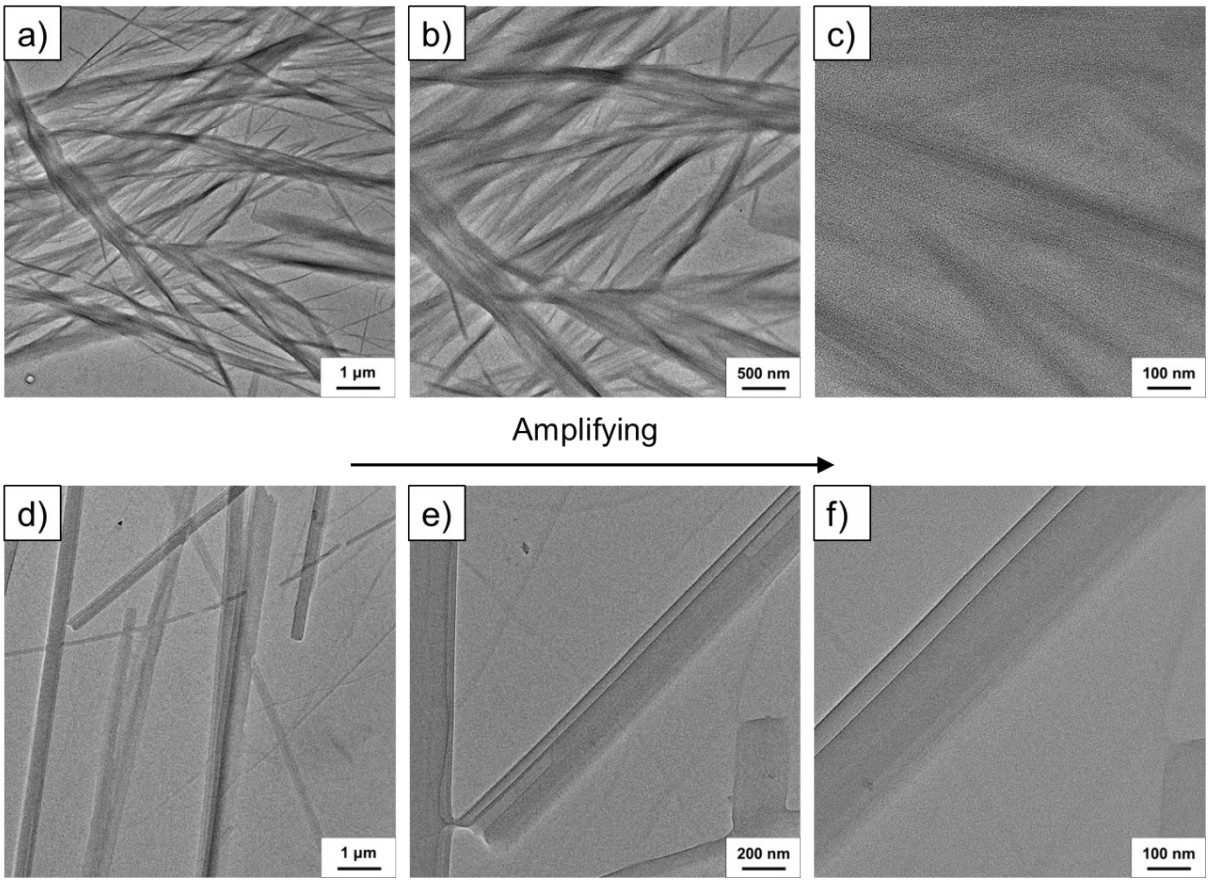

Figure S3. TEM images of primitive hydrogels with gradually increased magnification showing the (a-c) fine structure of fibrous aggregates in **Gel 1** that are composed of laterally stacked nanowires, and (d-f) the lack of ordered thinner components in ribbon-like aggregates of **Gel 2**.

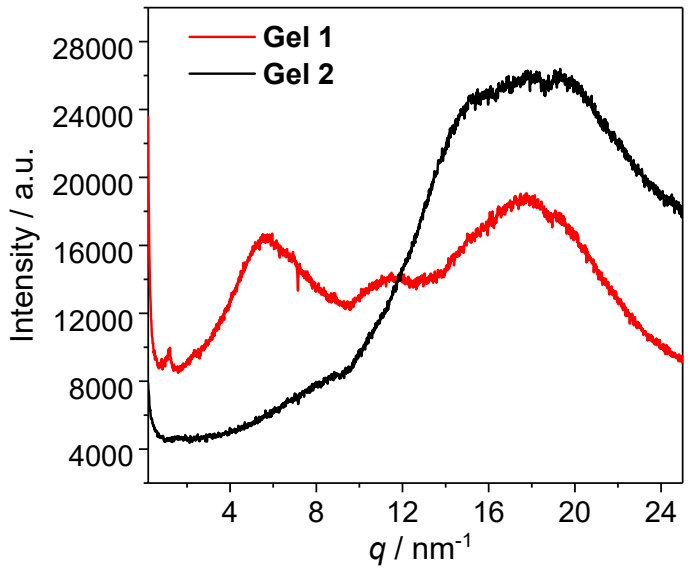

Figure S4. X-ray diffraction pattern of **Gel 1** and **Gel 2**.

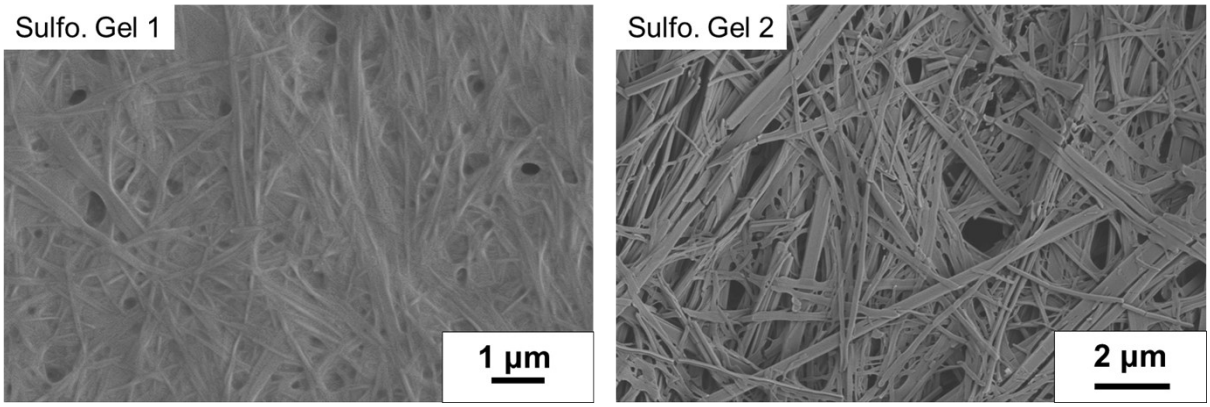

Figure S5. SEM images of peptide hydrogels co-assembled with Sulforhodamine B, showing that the microstructure of **Gel 1** (c_{NaOH} = 11 mM) and **Gel 2** (c_{NaOH} = 14 mM) are retained after incorporation of dyes (c_{Dye} = 0.16 mM).

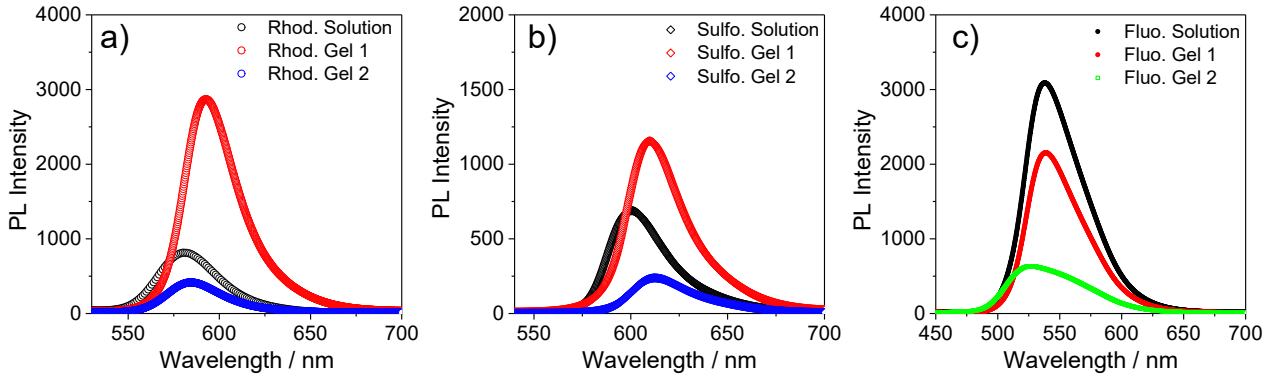

Figure S6. Comparison of fluorescence spectra for dye solution, dye-incorporated **Gel 1**, and dye-incorporated **Gel 2** at the same dye concentrations (Rhodamine B: c_{Dye} = 0.27 mM, Sulforhodamine B: c_{Dye} = 0.12 mM, Fluorescein sodium salt: c_{Dye} = 0.16 mM).

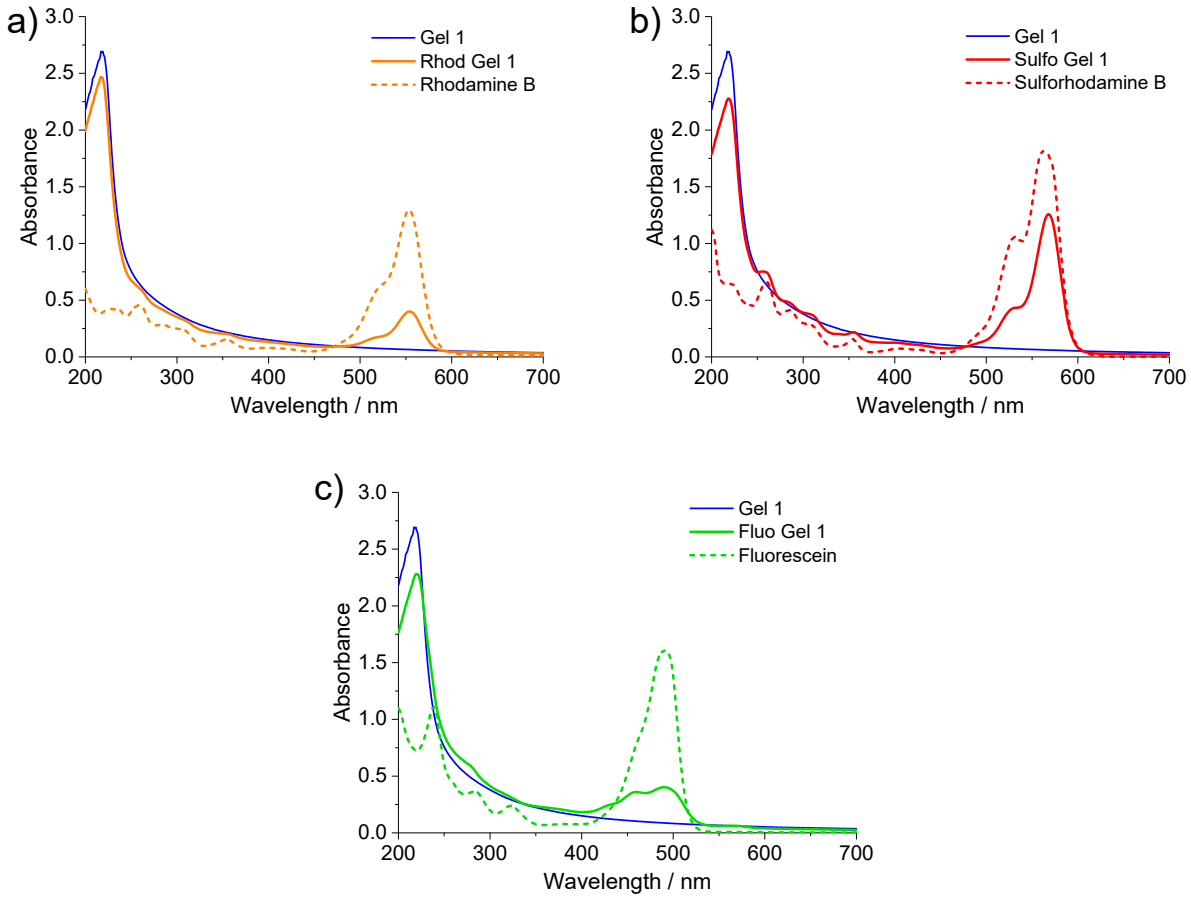

Figure S7. UV/Vis absorption spectra of primitive **Gel 1**, dye solutions, and co-assembled hybrid hydrogels (c_{Dye} = 0.16 mM).

Supporting discussion on the concentration-dependent fluorescence spectroscopy:

Under the presumption that positively charged dyes are associated to the periphery of nanowires in **Gel 1** through electrostatic interactions, the surface area of these nanowires should exert a limitation to the maximum amount of associated dye molecules. As a consequence, when excess amount of dye molecules is present, aggregation caused quenching would still occur. To verify this presumption, we further measured the fluorescence spectra of hybrid hydrogels containing varying concentrations of Rhodamine B or Sulforhodamine B dye molecules (Figure S8a, c). As a result, with the increase of dye concentration (c_{Dye}), the emission intensity of hydrogels ascended to a maximum value and then declined. In the meanwhile, the maximum emission wavelength of **Rhod. Gel 1** (**Sulfo. Gel 1**) was bathochromically shifted from 584 to 598 nm (597 to 625 nm) with the increase of c_{Dye}. The intensity of emission bands was plotted as a function of c_{Dye} (Figure S8b, d), and maximum values could be observed at c_{Dye} = 0.27 mM and c_{Dye} = 0.12 mM for **Rhod. Gel 1** and **Sulfo. Gel 1** respectively, which corresponds to the maximum amount of dye molecules associated to the periphery of **Gel 1** nanofibers. Moreover, the maximum emission intensity for **Sulfo. Gel 1** appears at lower concentration than for **Rhod. Gel 1**. This phenomenon is an additional validation for the proposed association pattern between dye molecules and nanofibers. Because the structure of Sulforhodamine B possesses two sulfonate groups which impose stronger electrostatic repulsion between adjacent dye molecules than a single carboxylate of Rhodamine B, it occupies larger area during the arrangement on the exterior surface of nanofibers. Therefore, a less amount of Sulforhodamine B molecules could be associated, and the maximum emission intensity is approached at a lower dye concentration.

For comparison, the concentration-dependent fluorescence spectra of **Fluo. Gel 1** (Figure S9) were also measured, in which the plot for the change of emission intensity displayed a very different shape. The maximum value is approached at a very low concentration (*ca*. 0.05 mM) and then declines with further increase of the concentration, which indicates the self-aggregation of anionic Fluorescein dyes due to lack of association with the nanofiber aggregates.

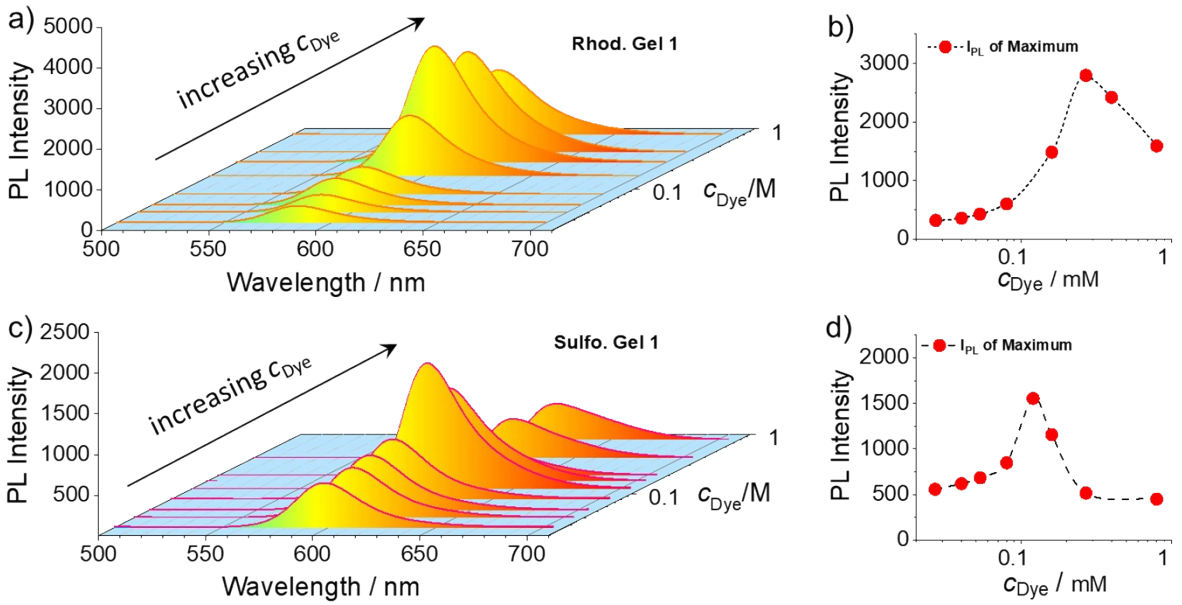

Figure S8. Fluorescence spectra of hybrid hydrogels containing varying concentrations of (a) Rhodamine B and (c) Sulforhodamine B dyes. Plots of fluorescence intensity at emission maximum as a function of dye concentration (c_{Dye}) for (b) Rhodamine B and (d) Sulforhodamine B. Dashed lines are guide for eyes.

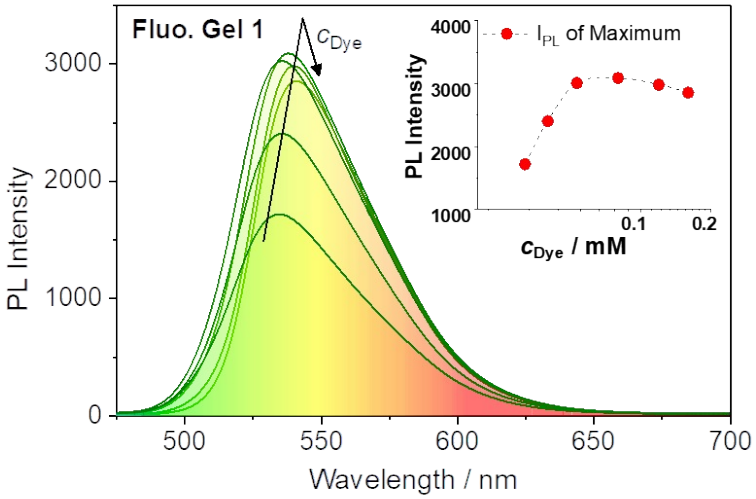

Figure S9. Fluorescence spectra of **Fluo. Gel 1** containing varying concentrations of Fluorescein sodium salt. Inset is the plot of fluorescence intensity at emission maximum as a function of dye concentration (c_{Dye}). Dashed lines are guide for eyes.

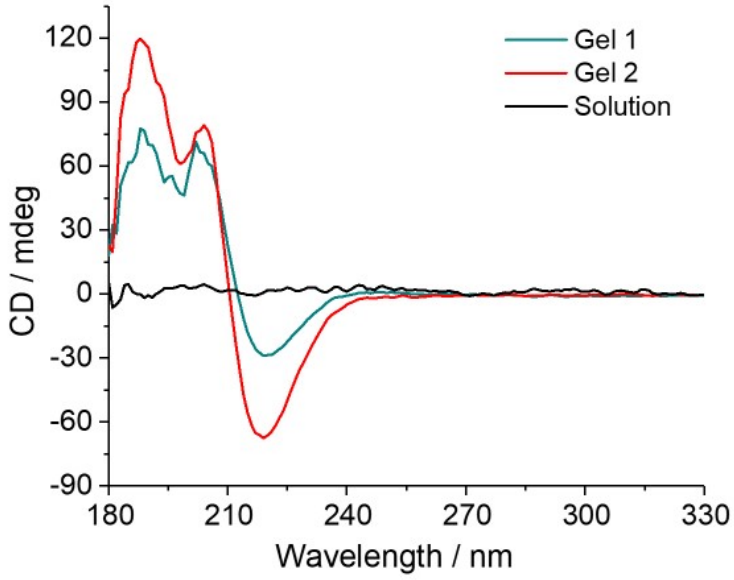

Figure S10. Circular dichroism spectra of the palmitoyl pentapeptide aqueous systems (c_{pep} = 8 mM) at different alkalinity: **Gel 1** (c_{NaOH} = 11 mM), **Gel 2** (c_{NaOH} = 14 mM), and solution (c_{NaOH} = 0).

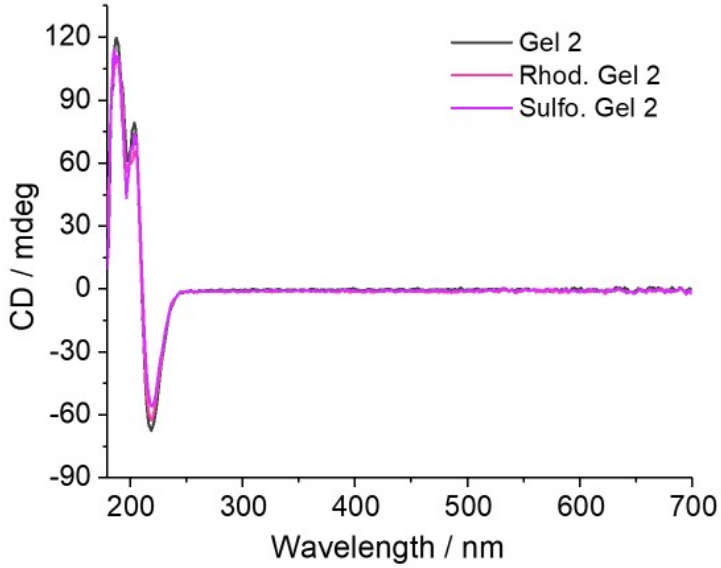

Figure S11. Circular dichroism spectra for hybrid hydrogels based on **Gel 2** (**Rhod. Gel 2**: c_{Dye} = 0.27 mM; **Sulfo. Gel 2:** c_{Dye} = 0.12 mM).

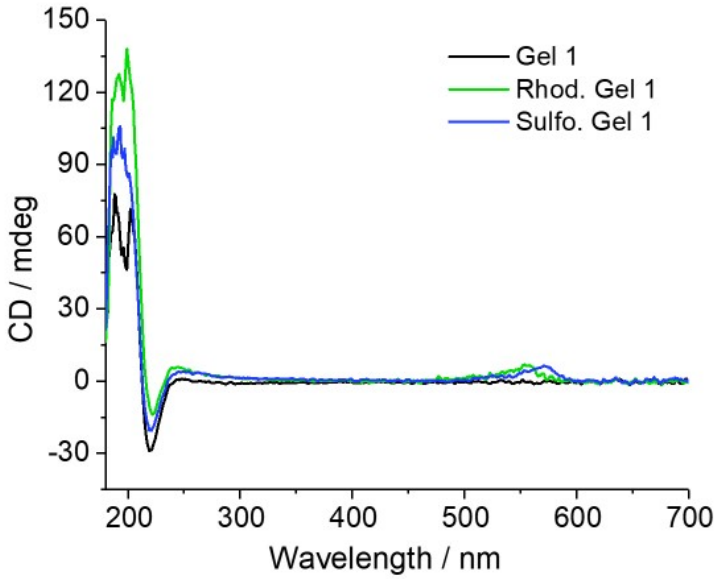

Figure S12. Circular dichroism spectra for hybrid hydrogels based on **Gel 1** (**Rhod. Gel 1**: c_{Dye} = 0.27 mM; **Sulfo. Gel 1:** c_{Dye} = 0.12 mM).